INTERNATIONAL JOURNAL OF AGRICULTURE & BIOLOGY
ISSN Print: 1560–8530; ISSN Online: 1814–9596
25–993/2026/35:350203
http://www.fspublishers.org

Full Length Article

Optimization of Conventional Extraction for Tyrosinase Inhibition and Modern Extraction for Elastase Inhibition of 70% Ethanol Extract of *Litsea oppositifolia* Stems

Bonita Risky Aprilenia, Sakinah, Donna Maretta Ariestanti and Berna Elya*
Department of Pharmacognosy and Phytochemistry, Faculty of Pharmacy, Universitas Indonesia, Depok 16424, Indonesia
*For correspondence: berna.elya@farmasi.ui.ac.id
Received 20 September 2025; Accepted 20 October 2025; Published online 09 November 2025

Editor: Abdul Wahid

Abstract

Litsea oppositifolia Gibbs, an Indonesian plant with significant antioxidant properties, shows potential for combating UV-induced skin aging. Still, crucial scientific data regarding its characteristics and optimal extraction for inhibiting elastase and tyrosinase enzymes remain limited. Therefore, the present study aimed to conduct a microscopic characterization of the *L. oppositifolia* stem, compare the efficacy of conventional and modern extraction techniques, and evaluate the potential of the resulting ethanolic extracts as dual inhibitors of elastase and tyrosinase for anti-photoaging applications. Microscopic and Scanning Electron Microscopy analyses of the *L. oppositifolia* stem successfully identified key characteristic fragments, including sclereids, fibers, and calcium oxalate crystals. Among the four extraction methods evaluated, reflux provided the highest extraction yield (5.22 ± 0.10%). In contrast, maceration yielded the highest total flavonoid content (2.80 ± 0.42 mg equivalent/g extract), suggesting that high-temperature methods may degrade thermolabile compounds. Furthermore, the macerated extract demonstrated a dose-dependent but weak inhibitory effect against tyrosinase, achieving only 16.46 ± 1.00% inhibition at 600 μg/mL, which was substantially lower than the kojic acid positive control (IC_{50} = 5.55 μg/mL). Similarly, the ultrasound-assisted extraction showed modest, dose-dependent elastase inhibition, reaching 15.63 ± 0.08% at 60 μg/mL, significantly weaker than the quercetin positive control (IC_{50} = 4.88 μg/mL). These findings indicate that although *L. oppositifolia* exhibits relatively low anti-tyrosinase and anti-elastase activity, it still demonstrates potential as a natural candidate for anti-aging and skin pigmentation management, with maceration identified as the most effective extraction method.

Keywords: *L. oppositifolia*; Conventional extraction; Modern extraction; Total flavonoid; Tyrosinase inhibitor; Elastase inhibitor

Introduction

Long-term exposure to ultraviolet (UV) radiation is a main cause of skin damage (D'Orazio *et al*. 2013; Merin *et al*. 2022). UV light can produce reactive oxygen species (ROS), which activate enzymes like elastase and tyrosinase (Jager *et al.* 2017; Wei *et al*. 2024). Elastase can break down elastin, reducing skin elasticity and causing wrinkles (Tsuji *et al*. 2001), while tyrosinase can promote melanogenesis, leading to dark spots or hyperpigmentation (Thawabteh *et al.* 2023). These enzymes can speed up premature skin aging. For this reason, many studies are now focused on finding inhibitors of elastase and tyrosinase to help prevent skin aging and pigmentation problems (He *et al.* 2024).

Litsea oppositifolia Gibbs a species of Lauraceae family, has drawn interest because of its phytochemicals, particularly flavonoids, which are often linked with antioxidant properties (Li *et al*. 2024). Plants from the *Litsea* genus have long been used in traditional medicine to ease ailments such as coughs, colds, headaches and arthritis. However, the potential of *L. oppositifolia* to inhibit elastase and tyrosinase has yet to be studied. In addition, detailed microscopic data needed for the identification and standardization of this species are still lacking.

Recently our group extracted the stem of *L. oppositifolia* using 70% ethanol through maceration. The resulting extract demonstrated strong antioxidant activity in the 2,2-diphenyl-1-picrylhydrazyl (DPPH) assay, with a half maximal inhibitory concentration (IC_{50}) of 8.307 ± 0.04 μg/mL (Ariestanti *et al*. 2024). This strong antioxidant activity is presumably linked to high flavonoid content of the extract. Flavonoids, as phenolic compounds, are well known for their ability to neutralize reactive oxygen species (ROS) and free radicals generated during oxidative stress (Syahputra *et al*. 2024). By reducing oxidative damage, flavonoids may play a protective role against skin aging and

To cite this paper: Aprilenia BR, Sakinah, DM Ariestanti, B Elya (2026). Optimization of conventional extraction for tyrosinase inhibition and modern extraction for elastase inhibition of 70% ethanol extract of *Litsea oppositifolia* stems. *Intl J Agric Biol* 35:350203. https://doi.org/10.17957/IJAB/15.2433

hyperpigmentation as potential inhibitors of elastase and tyrosinase. Hence, in the present study, we further investigated *L. oppositifolia* stem extract as an anti-tyrosinase and elastase, which can be potentially utilised as an anti-aging and pigmentation-regulating agent.

However, prior studies have been limited to conventional extraction methods such as maceration. To the best of the author's knowledge, no investigations have addressed the influence of extraction techniques, whether conventional extraction, including maceration and reflux, or modern methods, including ultrasound-assisted extraction (UAE) or microwave-assisted extraction (MAE), on extraction efficiency, the profile of bioactive compounds, and elastase and tyrosinase inhibitory activity.

Therefore, the present work was aimed at to characterize the *L. oppositifolia* stem by microscopic analysis of the *L. oppositifolia* stem, investigate the effects of conventional and non-conventional extraction methods, and evaluate the potential of its ethanolic extracts as inhibitors of elastase and tyrosinase activity.

Materials and Methods

Experimental details and treatments

Plant material: The plant material used in this research consisted of the stems of *L. oppositifolia*. The plant material was obtained from the Bogor Botanical Gardens in West Java, Indonesia. Taxonomic identification was conducted and confirmed at the Research Center for Plant Conservation and Botanic Gardens, Indonesian Institute of Sciences (LIPI) (Sample No: B-1612/IPH.3/KS/V/2019). The plant material is stored at the Faculty of Pharmacy, Universitas, Indonesia.

In the present study, we examined *L. oppositifolia* stems extract for anti-tyrosinase and elastase. Prior to the extraction process, the sample was air-dried. The air-drying technique was utilised to minimise the loss of secondary metabolites that are prone to degradation upon exposure to elevated temperatures or direct sunlight. Furthermore, the reduction in particle size increases the total surface area of the stem, which facilitates solvent penetration during the extraction process more effectively.

Chemicals: Chemicals used in this study were 3,4-Dihydroxy-L-phenylalanine (L-DOPA) (Sigma Aldrich, USA), aluminum chloride, chloral hydrate, dimethyl sulfoxide (DMSO), distilled water, ethanol (analytical grade), hydrochloric acid, kojic acid (Sigma Aldrich, USA), mushroom tyrosinase enzyme (Sigma Aldrich, USA), N-succinyl-(Ala)3-p-nitroanilide (SANA) substrate (Sigma Aldrich, USA), Porcine Pancreatic Elastase (PPE) E1250 (Sigma Aldrich, USA), potassium dihydrogen phosphate, quercetin (Sigma Aldrich, USA), sodium acetate, sodium hydroxide, and Trizma® base (Sigma Aldrich, USA).

Characterization of *L. oppositifolia*: *L. oppositifolia* stem powder was characterized to verify its identity. The evaluation included macroscopic analysis and microscopic examination using a light microscope (Nikon Eclipse E200, Japan) and a scanning electron microscope (SEM). The *L. oppositifolia* stem powder was dropped with the 70% chloral hydrate solution and then gently warmed prior to the observation under a light microscope. Moreover, *L. oppositifolia* stem powder was further examined under SEM with 130X and 500X magnifications.

Extraction: Stems of *L. oppositifolia* were first sorted, cleaned, and then air-dried at room temperature for approximately one week. Then, the dried stem was ground using a mechanical grinder to obtain a fine powder (Fig. 1). To determine an optimal extraction procedure, we compared two traditional methods (maceration and reflux) with two modern techniques, which are UAE and MAE (Bitwell *et al.* 2023). All extraction methods were conducted in five replications. The extract was used for characterization by microscopic examination and the extraction process

Maceration: The extraction was performed using three cycles of cold maceration with 10 g of stem powder. In each cycle, the powder was mixed with 70% ethanol (1:10 w/v) and left for 24 h, with occasional shaking. After each cycle, the liquid was collected, and the remaining powder was treated with fresh ethanol for the next cycle. When all cycles were finished, the liquids were combined, filtered, and the ethanol was removed using a rotary evaporator (Buchi Rotavapor-205, Switzerland) and a water bath to obtain the crude extract (Ariestanti *et al*. 2024).

Reflux: Reflux extraction was conducted in three cycles. In each cycle, 10 g of stem powder were heated with 70% ethanol (1:10 w/v) at 80°C for 1 h. Fresh solvent was used for each cycle. After all cycles were finished, the liquids were combined, filtered, and the ethanol was removed using a rotary evaporator (Buchi Rotavapor-205, Switzerland) and a water bath to obtain the crude extract (Xing and Wang 2021).

Ultrasound-assisted extraction (UAE): For the UAE method, 10 g of stem powder was mixed with 70% ethanol (1:30 w/v) and treated with ultrasound in three separate 30 min cycles. After sonication, the liquid extract was filtered, and the ethanol was removed using a rotary evaporator (Buchi Rotavapor-205, Switzerland) and a water bath to obtain the crude extract (Irawan *et al.* 2021).

Microwave-assisted extraction (MAE): For MAE method, 10 g of stem powder was mixed with 70% ethanol (1:30 w/v) and exposed to microwave energy at 70% power for 10 min in three cycles. After extraction, the liquid was filtered, and the ethanol was removed using a rotary evaporator (Buchi Rotavapor-205, Switzerland) and a water bath to obtain the crude extract (XiaoGeng *et al.* 2001).

Evaluation of 70% ethanol extract of *L. oppositifolia* stems

Extraction yield: The yield of crude extract obtained from each extraction method was calculated using the equation of Ngamkhae *et al.* (2022):

$$\text{Extraction yield (\%)} = \frac{Obtained\ extract\ weight\ from\ each\ method}{Litsea\ oppositifolia\ Gibbs\ stems\ powder\ weight} \times 100\% \quad (1)$$

Fig. 1: Macroscopic observation of *L. oppositifolia* stem powders

Determination of total flavonoid content: The total flavonoid content was measured using the aluminium chloride colorimetric method, with quercetin as the reference standard (Ditjen 2017; Shraim *et al.* 2021). Quercetin was prepared in ethanol at concentrations of 3–9 μg/mL. For the samples, 0.15 g of extract was dissolved in ethanol, sonicated for 30 min, and filtered. Then, 0.5 mL of the sample solution was mixed with 1.5 mL of ethanol, 0.1 mL of 10% aluminium chloride, 0.1 mL of 1 *M* sodium acetate and 2.8 mL of distilled water. The mixtures were vortexed and left at room temperature for 30 min before measuring the absorbance at 438 nm using a UV–Vis spectrophotometer T80+ (PG Instruments Ltd., UK) (Sembiring *et al.* 2018; Ladeska *et al.* 2022; Nicolescu *et al.* (2025). The total flavonoid content was calculated using the following expression.

$$\text{Total flavonoid content (mg equivalent/g sample)} = \frac{\text{quercetin equivalent concentration } (\mu g/\text{mL}) \times \text{dilution factor} \times \text{volume (mL)}}{\text{extract weight (g)} \times 1000} \quad (2)$$

In vitro bioactivity assay

The inhibitory activity of the 70% ethanol stem extract was then tested against both tyrosinase and elastase. The extract prepared via maceration was used for the anti-tyrosinase assay, whereas the anti-elastase assay utilised the extract obtained through UAE.

Inhibition assay for tyrosinase activity: The tyrosinase enzyme concentration was optimized within the range of 75–333 U/mL, while the L-DOPA substrate concentration was measured between 1 and 6.5 m*M*. The reaction was conducted by adding 120 μL of 0.5 m*M* phosphate buffer (pH 6.5), 40 μL of L-DOPA solution and 40 μL of tyrosinase solution into each well of a microplate. The mixture was subsequently incubated for 30 min at 25°C and agitated for 60 sec before the measurement at 490 nm with the microplate reader (VersaMax, Molecular Devices, USA).

For the tyrosinase inhibition assay, a reaction mixture was prepared in each well by adding 80 μL of 50 m*M* phosphate buffer (pH 6.5), 40 μL of 4 m*M* L-DOPA solution, and 40 μL of 75 U/mL tyrosinase solution. To this mixture, 40 μL of either kojic acid solution (final concentrations of 4–12 μg/mL) or the extract solution (final concentrations of 300 and 600 μg/mL) was added and then incubated for 30 min at 25°C, followed by agitation for 60 sec. The absorbance was measured at 490 nm using a microplate reader (VersaMax, Molecular Devices, USA). A sample control (without tyrosinase) and a blank (without enzyme and sample) were also measured. All experiments were conducted in triplicate (Ambarwati *et al.* 2021, 2022). The percentage of tyrosinase inhibition was calculated using the following expression.

$$\text{Inhibition (\%)} = \frac{\text{Absorbance of (Blank - blank without enzyme) - (Sample - sample without enzyme)}}{\text{Absorbance of (Blank - blank without enzyme)}} \quad (3)$$

Inhibition assay for elastase activity: Before the inhibition assay, the porcine pancreatic elastase (PPE) concentration, SANA substrate concentration, and incubation time were optimised. The amount of enzyme was added to 200 μL Tris-HCl buffer (pH 8) with final concentrations of 0.0110–0.0330 U/mL and then incubated at 25°C for 20 min. The SANA substrate was then added to achieve final concentrations of 0.0650–0.2275 m*M* and incubated for 30 min at 25°C. For incubation time optimisation, Tris-HCl buffer and 0.22 U/mL enzyme were added, followed by 1.3 m*M* SANA substrate, and incubated at 25°C for 5–60 min. Absorbance was measured at 405 nm using a microplate reader (VersaMax, Molecular Devices, USA).

For elastase inhibition assay, 30 μL of quercetin (final concentrations 1.5 – 13.5 μg/mL) or sample (final concentrations 15 and 60 μg/mL) was added to 120 μL of 100 m*M* Tris-HCl buffer (pH 8) and 20 μL of porcine pancreatic elastase (0.22 U/mL) in each well, followed by incubation at 25°C for 20 min. Subsequently, 30 μL of 1.3 m*M* SANA substrate was added and incubated for an additional 50 min. Absorbance was measured at 405 nm using a microplate reader (VersaMax, Molecular Devices, USA). A sample control was prepared for each test concentration without the enzyme, and a blank control was prepared without both elastase and the test sample. All experiments were performed in three replications. The percentage of elastase inhibition was calculated using Eq. 3 (Desmiaty *et al.* 2018; Kim *et al.* 2016).

Statistical Analysis

To determine the significance of each parameter, extraction yield and total flavonoid content data were analysed by using GraphPad Prism 9.0 with a one-way analysis of variance (ANOVA) followed by a Tukey HSD post hoc test.

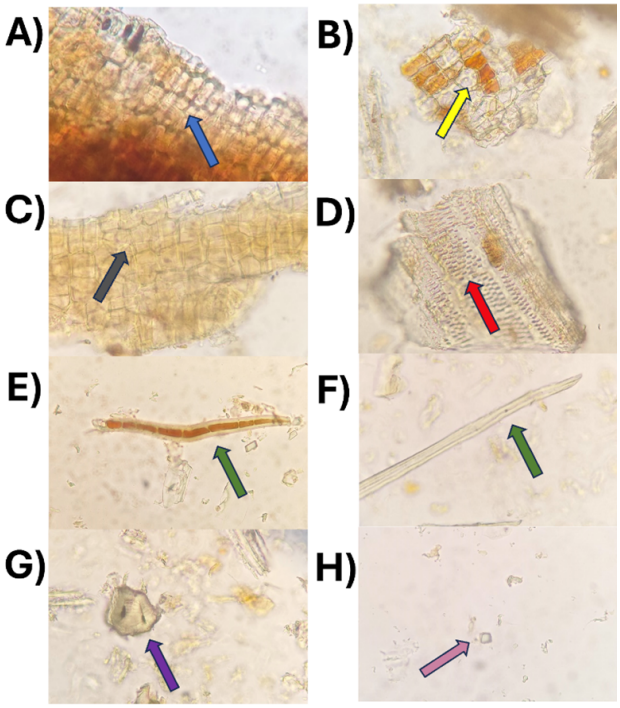

Fig. 2: Microscopic observation of *L. oppositifolia* stems powder by using an optical microscope. (**A**) Epidermis (blue arrow), (**B**) Parenchyma containing orange pigment (yellow arrow), (**C**) Cork cells (grey arrow), (**D**) Vascular bundle with pitted thickening (red arrow), (**E**–**F**) Fibers (green arrow), (**G**) Stone cells (sclereids) (purple arrow) and (**H**) Prismatic calcium oxalate crystals (pink arrow)

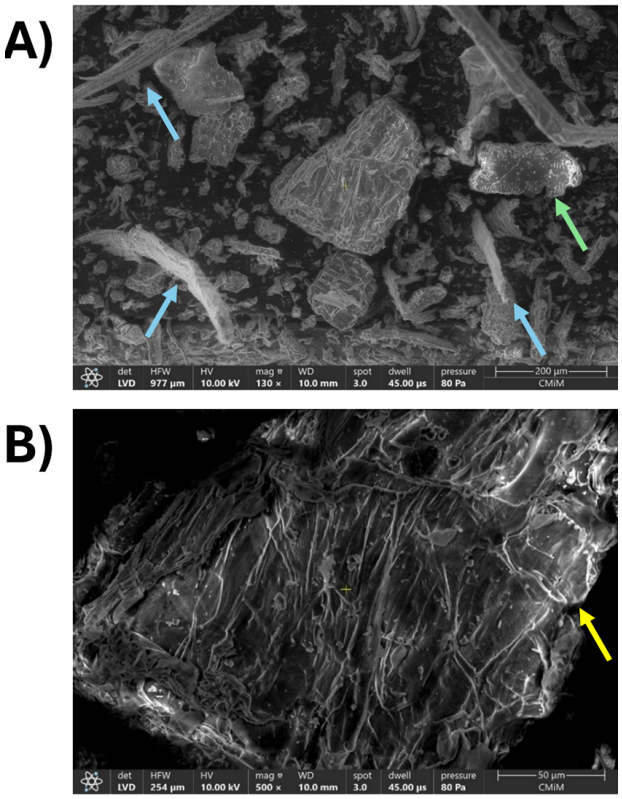

Fig. 3: Microscopic observation of *L. oppositifolia* stems by using a scanning electron microscope. (**A**) fibers (blue arrow) and sclereids (green arrow) within 130X magnification and (**B**) parenchyma cells (yellow arrow) within 500X magnification

For the tyrosinase and elastase inhibition assay, data were analysed using a two-tailed Student's *t*-test with GraphPad Prism 9.0. The data were expressed as the mean ± SD. A < 5% probability showed a significant difference between the groups.

Results

Characterization of *L. oppositifolia*

The *L. oppositifolia* stems were sorted, cleaned, and air-dried at room temperature for approximately one week. Subsequently, the *L. oppositifolia* stems were ground into a powder using a mechanical grinder. The grinding process produced a fine, brown powder from the *L. oppositifolia* stems.

The optical microscope imaging confirmed the specific fragments of the *L. oppositifolia* stem, which can be utilised as identification and standardisation (Fig. 2). In the outermost layer, the epidermal tissue with rectangular cells was identified (Fig. 2A). Moreover, parenchymatous tissue was found to be orange-brown pigmented cells (Fig. 2B). Furthermore, the periderm was represented by quadrangular and pentagonal layers of cork cells with morphologies (Fig. 2C). In addition, the vascular bundles observed had thickened dots (Fig. 2D) and the fibers containing brownish pigments were observed in Fig. 2E–F. The microscopic analysis further revealed the presence of stone cells or sclereids with highly thickened and lignified walls (Fig. 2G), as well as prismatic calcium oxalate crystals (Fig. 2H).

The microscopic analysis of the *L. oppositifolia* stem was further performed under SEM to investigate the detailed fragments. The photographs revealed several key tissue types with distinct morphological characteristics, including fiber, parenchyma, and sclereids. Fiber fragments were characterized by an elongated morphology with tapering ends and were observed to be arranged both individually and in clusters (Fig. 3A with blue arrow). Moreover, the ground tissue was composed predominantly of parenchyma, characterized by thin-walled cells containing various organic and inorganic compounds, as indicated by pinkish-colored patches (Fig. 3B with yellow arrow). Among the parenchyma cells are clusters of sclereids with irregular morphology, varying in size, and having heavily lignified secondary walls (Fig. 3A with green arrow).

Extraction of *L. oppositifolia*

In this present study, we examined the extraction process, both conventional and modern extraction, on the extraction yield. As shown in Fig. 4, the reflux method exhibited a significantly higher ($P < 0.05$) extraction yield (5.22% ± 0.10%) compared to maceration (4.64% ± 0.35%) and

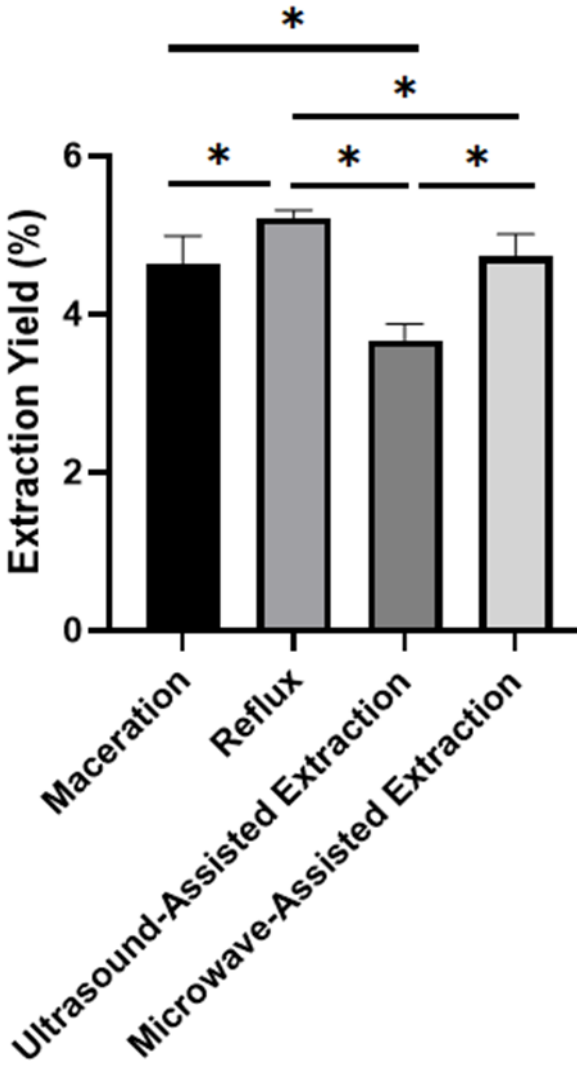

Fig. 4: Extraction yield of 70% ethanol of *L. oppositifolia* Stems. Data represent mean ± SD (n = 5). *) $P < 0.05$ represents a significant difference between groups

modern extraction processes. Moreover, MAE exhibited a significantly higher ($P < 0.05$) extract yield (4.73% ± 0.28%) compared to UAE (3.67% ± 0.20%) ($P < 0.05$).

Total flavonoid content of *L. oppositifolia*

The determination of total flavonoid content in the stem of *L. oppositifolia* was quantified using the aluminum chloride colorimetric method, by using quercetin at the maximum absorbance wavelength (λ max) of 438 nm (Fig. 5A). This wavelength was subsequently used for further measurements. The data from the calibration curve yielded a linear regression equation of y = 0.0756x + 0.0108, with a high correlation coefficient (r^2) of 0.9994 (Fig. 5B).

The total flavonoid content in the 70% ethanolic stem extract of *L. oppositifolia* was slightly higher when using the maceration method (2.80 ± 0.42 mg equivalent/g

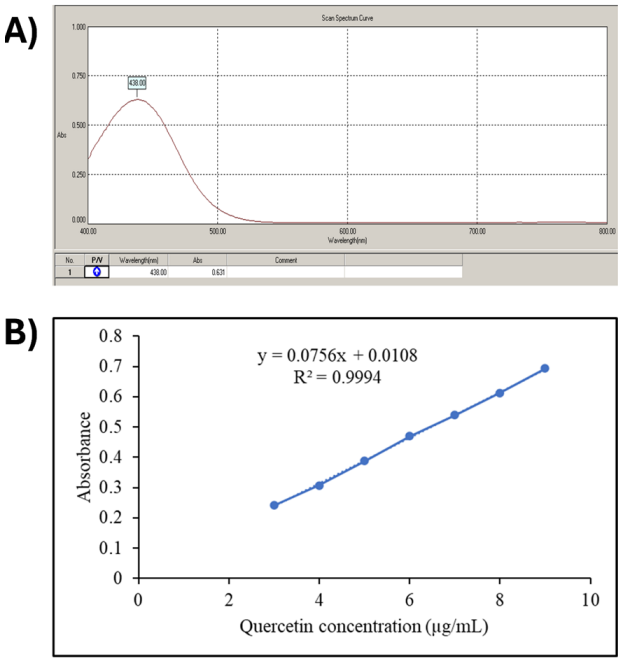

Fig. 5: UV-Vis analysis of quercetin standard for total flavonoid content determination. (**A**) Absorption spectrum and (**B**) Calibration curve of quercetin standard solution at 438 nm

extract) compared to the reflux and UAE methods (Fig. 6). The reflux extraction exhibited only 2.61 ± 0.06 mg equivalent/g extract. Furthermore, the modern extraction methods showed a lower value compared to the conventional methods, both maceration and reflux. UAE showed only 2.39 ± 0.03 mg equivalent/g extract; whereas MAE exhibited 1.69 ± 0.01 mg equivalent/g extract ($P < 0.05$).

Inhibition assay for tyrosinase activity of 70% ethanol extract of *L. oppositifolia* by using the conventional extraction methods

A preliminary tyrosinase enzyme assay was conducted to determine the optimal conditions between the tyrosinase enzyme and L-DOPA substrate. The enzyme concentration was optimized in the range of 75–333 U/mL, with only 75 U/mL yielding an absorbance within the range of 0.2–0.8 nm (Fig. 7A). Therefore, this concentration was selected for the tyrosinase inhibition assay on the positive control and samples. Furthermore, the L-DOPA substrate concentration was optimized in the range of 1– 6 m*M* using 75 U/mL of tyrosinase enzyme. According to Fig. 7B, the absorbance gradually increased at 1 to 3 m*M*, whereas no significant change was observed at 4 to 6 m*M*, indicating that the enzyme was saturated with substrate and the reaction rate had reached a steady-state condition.

To evaluate the tyrosinase inhibition assay, kojic acid was used as a positive control due to its well-characterized competitive inhibitor of tyrosinase. Based on Fig. 7C, kojic acid at concentrations of 4–12 μg/mL produced an IC_{50} of

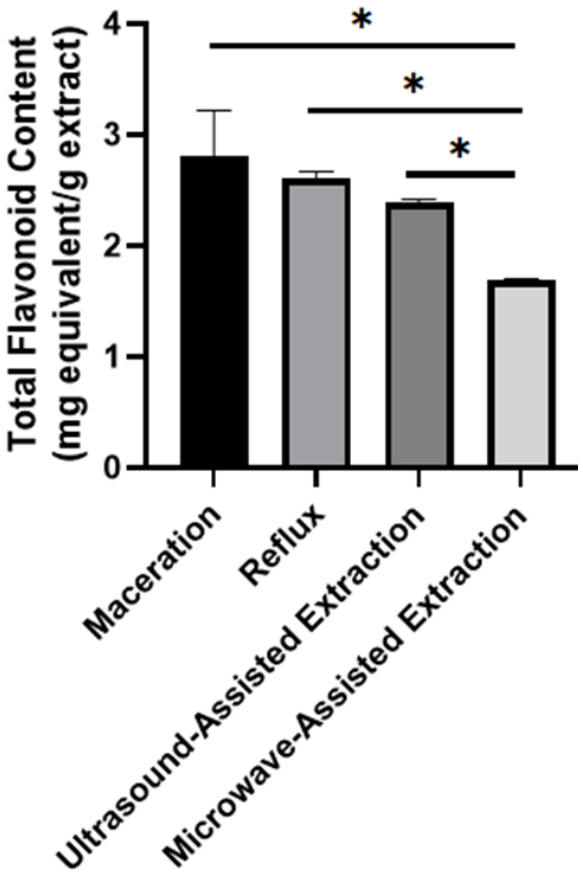

Fig. 6: Total flavonoid content of 70% Ethanol of *L. oppositifolia* Stems. Data represent mean ± SD (n = 3). * $P < 0.05$ represents a significant difference between groups

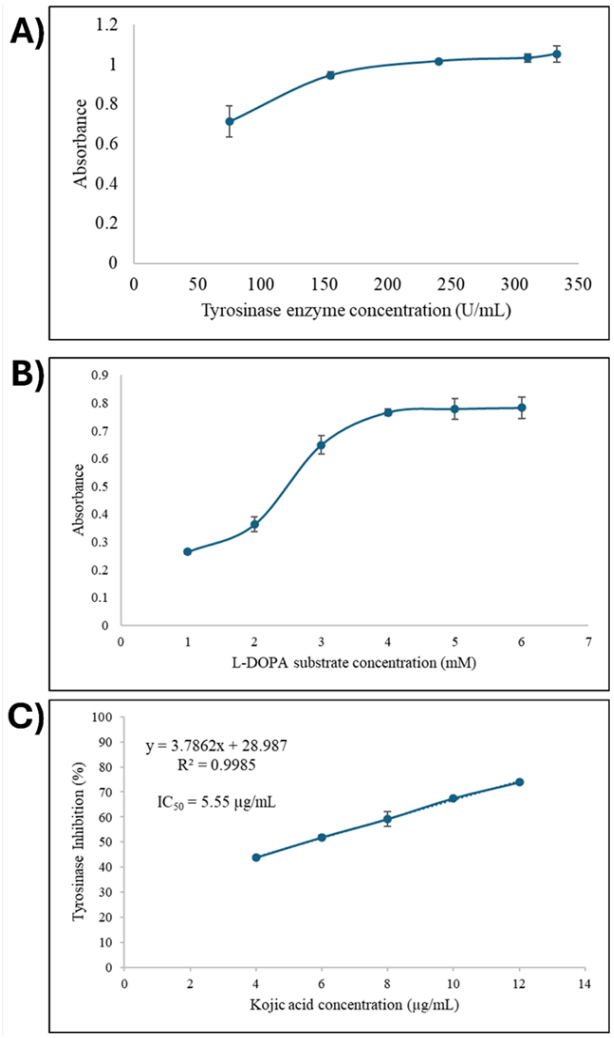

Fig. 7: Optimization of tyrosinase inhibition assay. (**A**) Enzyme concentration optimization with L-DOPA 3 m*M*, (**B**) L-DOPA optimization with enzyme tyrosinase 75 U/mL and (**C**) Tyrosiase inhibition by kojic acid. Data represents mean ± SD (n = 3)

5.55 μg/mL ($R^2 = 0.9985$), demonstrating its strong inhibitory effect on tyrosinase activity. Present work revealed that 70% ethanolic stem extract of *L. oppositifolia*, obtained through the maceration, exhibited a significant and dose-dependent inhibitory effect against tyrosinase (Table 1). A twofold increase in concentration of extract from 300–600 μg/mL resulted in enhanced enzymatic inhibition from 8.62 ± 0.65% to a statistically significant 16.46 ± 1.00% ($P < 0.05$).

Inhibition assay for elastase activity of 70% ethanol extract of *L. oppositifolia*. by using the conventional extraction methods

The preliminary elastase enzyme assay included the optimization of enzyme concentration, substrate concentration, and incubation time. Optimization of porcine pancreatic elastase enzyme concentration in the range of 0.0110–0.0330 U/mL showed a progressive increase in absorbance, with the optimum concentration determined at 0.022 U/mL (Fig. 8A). Moreover, the optimization of SANA substrate concentration was carried out in the range of 0.0650 – 0.2275 m*M*. The absorbance increased significantly up to 0.1950 m*M*, after which, a decline was observed at higher concentrations, indicating enzyme saturation by the substrate (Fig. 8B). Therefore, the substrate concentration of 0.195 m*M* was determined as the optimum substrate concentration. Additionally, optimization of incubation time was performed using the previously determined optimal concentrations of enzyme (0.022 U/mL) and substrate (0.195 m*M*). Fig. 8C showed that the absorbance increased progressively with incubation time, showing a significant rise between 10–50 min and reaching a plateau at 55 min. Therefore, 50 min was selected as the optimum incubation time for the elastase inhibition assay.

Elastase inhibition by quercetin, as the positive control, was evaluated at various concentrations, ranging from 1.5 to 13.5 μg/mL. The elastase inhibition assay revealed that quercetin has an IC_{50} value of 4.8816 μg/mL, indicating strong inhibitory activity (Fig. 8D). Elastase inhibition by 70% ethanolic extract of *L. oppositifolia* stem was evaluated using the UAE extract, which had the highest

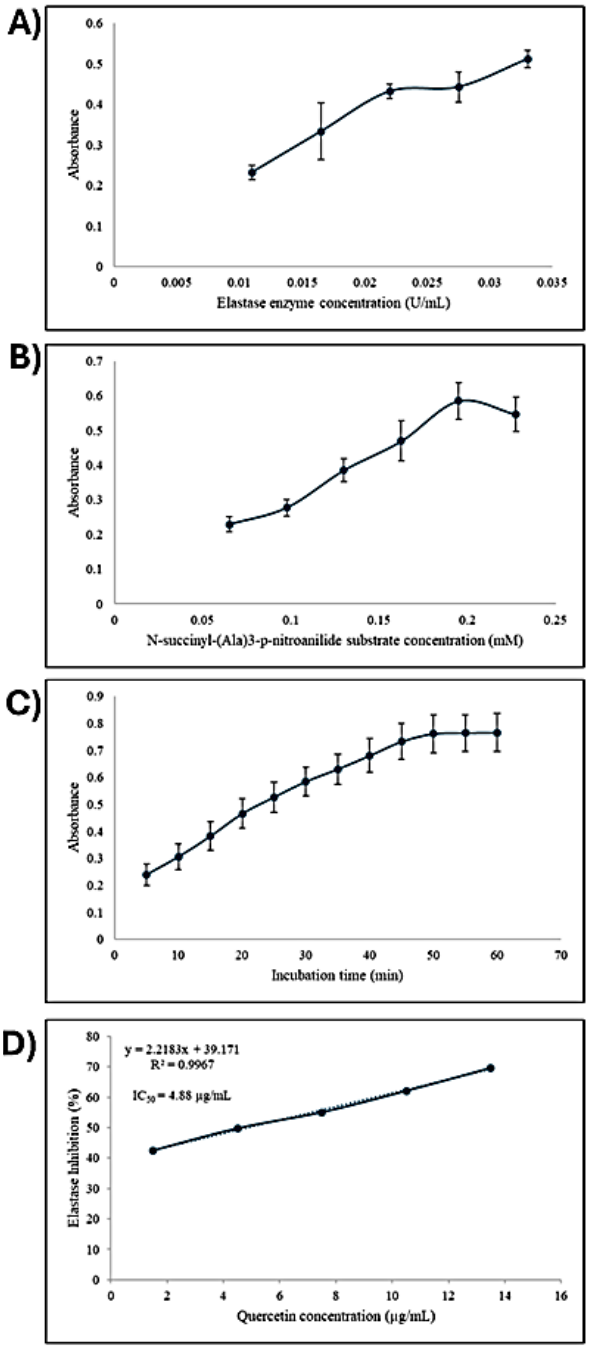

Fig. 8: Optimization of the elastase inhibition assay. (**A**) enzyme concentration optimization at incubation time of 30 mins, (**B**) substrate N-succinyl-(Ala)3-p-nitroanilide optimization at incubation time of 30 mins, (**C**) incubation time optimization with 0.1950 m*M* substrate and (**D**) elastase inhibition by quercetin. Data represents mean ± SD (n = 3)

flavonoid content. The assay was performed at 15 and 60 μg/mL, demonstrating a statistically significant ($P < 0.05$) and dose-dependent inhibitory effect on elastase activity, with elastase inhibition of 11.78 ± 0.60 and 15.63 ± 0.08%, respectively (Table 2).

Table 1: Tyrosinase inhibition assay of 70% ethanol extract of *L. oppositifolia* from the maceration method. Data represents mean ± SD (n = 3)

Extract concentration (μg/mL)	Tyrosinase inhibition (%)
300	8.62 ± 0.65*)
600	16.46 ± 1.00*)

*) $P < 0.05$ represents a significant difference between groups

Table 2: Elastase inhibition assay of 70% ethanol extract of *L. oppositifolia* from ultrasound-assisted extraction. Data represents mean ± SD (n = 3)

Extract concentration (μg/mL)	Elastase inhibition (%)
15	11.78 ± 0.60*)
60	15.63 ± 0.08*)

*) $P < 0.05$ represents a significant difference between groups

Discussion

The microscopic images showed specific fragments of the *L. oppositifolia* stem compared to other species. Epidermis, parenchyma, and vascular bundles were observed only in *L. oppositifolia,* whereas starch grains were only found in *L. chinensis* (Aeri *et al.* 2020). Stone cells, fibers, and calcium oxalate crystals, however, were present in both species. The microscopic images showed specific fragments in *L. oppositifolia* stem compared to other species. Epidermis, parenchyma, and vascular bundles were observed only in *L. oppositifolia*, whereas starch grains were only found in *L. chinensis* (Aeri *et al*. 2020). Stone cells, fibers, and calcium oxalate crystals, however, were present in both species.

Maceration and reflux were conducted as conventional methods to extract the stem powder of *L. oppositifolia* because of their simplicity and cost-effectiveness compared to modern techniques. In addition, we also tested modern extraction methods, MAE and UAE, which are faster and more efficient (Bitwell *et al*. 2023). In our previous study, we found that flavonoids and phenolic compounds are the main antioxidants in the stem of *L. oppositifolia*. Because 70% ethanol dissolves flavonoids well and is safe for traditional medicine use, we used it as the extraction solvent (Plaskova and Mlcek 2023).

Reflux extraction showed the highest yield. Higher temperature in the reflux can enhance the extraction of secondary metabolites from plant matrix cells to the solvent. The lower viscosity and surface tension also help the compounds move into the solvent more easily (Mungwari *et al*. 2025). In our study, MAE exhibited a higher yield than UAE because microwaves provide more energy to break the plant cell walls. Both MAE and UAE produce heat, which stimulates the compounds to diffuse into the solvent (Chaves *et al.* 2020). However, excessive localized heating may also accelerate the degradation of flavonoids.

In the present study, maceration exhibited the highest flavonoid content, probably because the room temperature can preserve flavonoid stability (Gao *et al*. 2022; Tourabi *et al*. 2025). Conversely, the reduced flavonoid content in other methods can be caused by thermal

degradation (Gao *et al*. 2022). In addition, localized high-energy ultrasound and microwave can further degrade flavonoid content in the extract (Biesaga 2011). Hence, we further investigated the highest flavonoid content for conventional and modern extraction for the *in vitro* bioactivity assay. The maceration extract was further studied for the tyrosinase inhibition assay, whereas the elastase inhibition was evaluated using the UAE extract.

Inhibition of tyrosinase activity was quantified by the accumulation of dopachrome from the enzymatic conversion of L-tyrosine to L-DOPA. The quantification of dopachrome was measured by using UV/Vis spectrophotometric absorbance at 490 nm (Fan *et al*. 2021) utilizing kojic acid as a positive control due to its ability to prevent the hydroxylation of L-tyrosine and the oxidation of L-DOPA to dopaquinone (Wang *et al*. 2022). *L. oppositifolia* stem extract showed a lower tyrosinase inhibition compared to kojic acid due to the presence of insufficient hydroxyl groups to stabilize the active site of tyrosinase. Another study revealed that rooibos (*Aspalathus linearis*) and longan peel (*Dimocarpus longan*) extracts display only weak tyrosinase inhibitory activity, achieving only around 7% at 500 μg/mL and 19.5 ± 0.6% at 100 μg/mL, respectively, despite their abundance of potent antioxidants such as phenolics and flavonoids (Momtaz *et al*. 2008; Prasad *et al.* 2010). This could be because there are not enough hydroxyl groups to make strong bonds with the active site of the enzyme, which can change the conformation of tyrosinase (Liu *et al*. 2022). Interestingly, although the ethanolic extract of *Sargassum polycystic* did not block mushroom tyrosinase, it was still able to reduce tyrosinase activity and melanin production in B16F10 cells. In contrast, melanocyte tyrosinase is membrane-bound, which strongly indicates that screening for skin-whitening agents is more reliable using melanocyte-derived tyrosinase compared to mushroom tyrosinase (Chan *et al*. 2011).

For the elastase inhibitor activity, we utilised quercetin as a positive control due to its non-competitive elastase inhibitory activity. The inhibition of elastase activity with 70% ethanolic stem extract of *L. oppositifolia* remained lower than that of quercetin. This result was supported by a study on *Citrus unshiu,* which showed that the fruit peels with the highest total flavonoid content had very low anti-elastase activity of 1–10% inhibition, while the flesh with lower flavonoid content exhibited significantly higher activity of 13–29% (Eun *et al.* 2020). This may be attributed to the complex composition of crude extracts, whose constituents may not specifically interact with the elastase enzyme. Effective inhibition of elastase activity requires the presence of a catechol moiety on the B-ring of flavonoids, which plays a key role in modulating their inhibitory potential (Popoola *et al*.2015).

Conclusion

Conventional maceration and reflux methods yielded higher total flavonoid content and better preservation of flavonoid compounds compared to modern techniques (UAE and MAE), with maceration providing the optimal balance of yield and total flavonoid content. Furthermore, the maceration extract exhibited significant, dose-dependent tyrosinase inhibition, with an increase from 8.62 ± 0.65% to 16.46 ± 1.00% at 300 to 600 μg/mL, respectively, despite being relatively lower than kojic acid (IC_{50} = 5.55 μg/mL). On the other hand, the UAE extract demonstrated a dose-dependent inhibition of the elastase enzyme with 11.78 ± 0.60% and 15.63 ± 0.08% suppression at concentrations of 15 and 60 μg/mL. However, its activity remained lower compared to quercetin (IC_{50} = 4.8816 μg/mL). These findings highlight the optimization of both conventional and modern extraction methods to maximize yield and bioactive potential for 70% ethanol *L. oppositifolia* stem extract, making it a promising candidate for future cosmeceutical applications.

Acknowledgements

The authors would like to acknowledge the Faculty of Pharmacy Universitas Indonesia for providing the research facilities.

Author Contributions

BRA, S, DMA and BE conceptualized the study and contributed to formal analysis. BRA and S designed the methodology, conducted the literature search and curated the data. BRA prepared the original draft. DMA and BE provided validation, supervision, and draft editing.

Conflict of Interest

The authors declare no conflicts of interest, financial or otherwise.

Data Availability

The authors state that all data relevant to the study's findings are presented within the article. Moreover, additional datasets produced or examined during the research can be accessed by contacting the corresponding author, subject to a reasonable request.

Ethics Approval

Not applicable to this study.

References

Aeri V, DB Narayana, D Singh (2020). *Litsea chinensis. In: Powdered Crude Drug Microscopy of Leaves and Barks*, pp:87–92. Vidhu A, DB Narayana, D Singh (Eds.). Elsevier, Amsterdam, Netherlands

Ambarwati NSS, MO Armandari, W Widayat, Y Desmiaty, B Elya, AE Arifianti, I Ahmad (2022). *In vitro* studies on the cytotoxicity, elastase, and tyrosinase inhibitory activities of tomato (*Solanum lycopersicum* Mill.) extract. *J Adv Pharm Technol Res* 13:182–186

Ambarwati NSS, B Elya, Y Desmiaty, AE Arifianti, I Ahmad (2021). Tyrosinase inhibitory activity of *Garcinia latissima* Miq. extracts.

Pharmacogn J 13:1673–1677

Ariestanti DM, B Elya, P Hartrianti, VC Arifin, C Hana, P Lovina, R Fadhila (2024). The anti-ageing potential of *L. oppositifolia* stem extract: Evidence from *in vitro* and *ex vivo* study on skin cell lines. *Farmacia* 72:521–531

Biesaga M (2011). Influence of extraction methods on stability of flavonoids. *J Chromatogr A* 1218:2505–2512

Bitwell C, SS Indra, C Luke, MK Kakoma (2023). A review of modern and conventional extraction techniques and their applications for extracting phytochemicals from plants. *Sci Afr* 19:01585

Chan YY, KH Kim, SH Cheah (2011). Inhibitory effects of *Sargassum polycystum* on tyrosinase activity and melanin formation in B16F10 murine melanoma cells. *J Ethnopharmacol* 137:1183–1188

Chaves JO, MCD Souza, LCD Silva, D Lachos-Perez, PC Torres-Mayanga, APDF Machado, T Forster-Carneiro, M Vázquez-Espinosa, AV González-de-Peredo, GF Barbero, MA Rostagno (2020). Extraction of flavonoids from natural sources using modern techniques. *Front Chem* 8:1-25

D'Orazio J, S Jarrett, A Amaro-Ortiz, T Scott (2013). UV radiation and the skin. *Intl J Mol Sci* 14:12222–12248

Desmiaty Y, W Winarti, AM Nursih, H Nisrina, G Finotory (2018). Antioxidant and antielastase activity of *Kaempferia rotunda* and *Curcuma zedoaria*. *Res J Chem Environ* 22:95–98

Ditjen Kefarmasian dan Alat Kesehatan (2017). *Farmakope Herbal Indonesia*, 2nd edn. Kementrian Kesehatan Republik Indonesia

Eun CH, MS Kang, IJ Kim (2020). Elastase/collagenase inhibition compositions of *Citrus unshiu* and its association with phenolic content and anti-oxidant activity. *Appl Sci* 10:1-11

Fan YF, SX Zhu, FB Hou, DF Zhao, QS Pan, YW Xiang, XK Qian, GB Ge, P Wang (2021). Spectrophotometric assays for sensing tyrosinase activity and their applications. *Biosensors* 11:1-22

Gao Y, W Xia, P Shao, W Wu, H Chen, X Fang, H Mu, J Xiao, H Gao (2022). Impact of thermal processing on dietary flavonoids. *Curr Opin Food Sci* 48:100915

He X, X Gao, Y Guo, W Xie (2024). Research progress on bioactive factors against skin aging. *Intl J Mol Sci* 25:1-19

Irawan C, B Elya, M Hanafi, FC Saputri (2021). Application of ultrasound-assisted extraction on the stem bark of *Rhinachantus nasutus* (L.) Kurz, total phenolic, and its potential as antioxidant and inhibitor of alpha-glucosidase enzyme activity. *Pharmacogn J* 13:1297–1303

Jager TLD, AE Cockrell, SSD Plessis (2017). Ultraviolet light induced generation of reactive oxygen species. *Adv Exp Med Biol* 996:15–23

Kim MJ, JM Hyun, SS Kim, KC Seong, CK Lim, JS Kang, SH Yun, KJ Park, HJ An, KS Park, YH Choi, NH Lee, CG Hyun (2018). *In vitro* screening of jeju island plants for cosmetic ingredients. *Orient J Chem* 32:807-815

Ladeska V, B Elya, M Hanafi, Kusmardi (2022). Antioxidants, total phenolic and flavonoid content and toxicity assay of ampelas (*Tetracera macrophylla* Wall.Ex Hook.F.& Thoms) from Kalimantan-Indonesia. *Pharmacogn J* 4:642–648

Li G, Z Li, Y Wang (2024). The genus *Litsea*: A comprehensive review of traditional uses, phytochemistry, pharmacological activities and other studies. *J Ethnopharmacol* 334:118494

Liu L, J Li, L Zhang, S Wei, Z Qin, D Liang, B Ding, H Chen, W Song (2022). Conformational changes of tyrosinase caused by pentagalloylglucose binding: Implications for inhibitory effect and underlying mechanism. *Food Res Int* 157:111312

Merin KA, M Shaji, R Kameswaran (2022). A review on sun exposure and skin diseases. *Ind J Dermatol* 67:1-8

Momtaz S, N Lall, A Basson (2008). Inhibitory activities of mushroom tyrosine and DOPA oxidation by plant extracts. *S Afr J Bot* 74:577–582

Mungwari CP, CK King'ondu, P Sigauke, BA Obadele (2025). Conventional and modern techniques for bioactive compounds recovery from plants: Review. *Sci Afr* 27:2509

Ngamkhae N, O Monthakantirat, Y Chulikhit, C Boonyarat, J Maneenet, C Khamphukdee, P Kwankhao, S Pitiporn, S Daodee (2022). Optimization of extraction method for kleeb bua daeng formula and comparison between ultrasound-assisted and microwave-assisted extraction. *J Appl Res Med Aromat Plants* 28:100369

Nicolescu A, CI Bunea, A Mocan (2025). Total flavonoid content revised: An overview of past, present, and future determinations in phytochemical analysis. *Anal Biochem* 700:115794

Plaskova A, J Mlcek (2023). New insights of the application of water or ethanol-water plant extract rich in active compounds in food. *Front Nutr* 10:1-23

Popoola OK, JL Marnewick, F Rautenbach, F Ameer, EI Iwuoha, AA Hussein (2015). Inhibition of oxidative stress and skin aging-related enzymes by prenylated chalcones and other flavonoids from *Helichrysum teretifolium*. *Molecules* 20:7143–7155

Prasad KN, B Yang, J Shi, C Yu, M Zhao, S Xue, Y Jiang (2010). Enhanced antioxidant and antityrosinase activities of longan fruit pericarp by ultra-high-pressure-assisted extraction. *J Pharm Biomed Anal* 51:471–477

Sembiring EN, B Elya, R Sauriasari (2018). Phytochemical screening, total flavonoid and total phenolic content and antioxidant activity of different parts of C*aesalpinia bonduc* (L.) Roxb. *Pharmacogn J* 10:123–127

Shraim AM, TA Ahmed, MM Rahman, YM Hijji (2021). Determination of total flavonoid content by aluminum chloride assay: A critical evaluation. *LWT Food Sci Technol* 150:1-11

Syahputra RA, A Dalimunthe, ZD Utari, P Halim, MA Sukarno, S Zainalabidin, E Salim, M Gunawan, F Nurolis, MN Park, JA Luckanagul, H Bangun, B Kim, U Harahap (2024). Nanotechnology and flavonoids: Current research and future perspectives on cardiovascular health. *J Functional Foods* 120:106355

Thawabteh AM, A Jibreen, D Karaman, A Thawabteh, R Karaman (2023). Skin pigmentation types, causes and treatment-A review. *Molecules* 28:1-28

Tourabi M, K Faiz, R Ezzouggari, B Louasté, M Merzouki, M Dauelbait, M Bourhia, KS Almaary, F Siddique, B Lyoussi, E Derwich (2025). Optimization of extraction process and solvent polarities to enhance the recovery of phytochemical compounds, nutritional content, and biofunctional properties of *Mentha longifolia* L. extracts. *Bioresour Bioproc* 12:1-18

Tsuji N, S Moriwaki, Y Suzuki, Y Takema, G Imokawa (2001). The role of elastases secreted by fibroblasts in wrinkle formation: Implication through selective inhibition of elastase activity. *Photochem Photobiol* 74:283–290

Wang W, Y Gao, W Wang, J Zhang, J Yin, T Le, J Xue, UH Engelhardt, H Jiang (2022). Kojic acid showed consistent inhibitory activity on tyrosinase from mushroom and in cultured B16F10 cells compared with arbutins. *Antioxidants* 11:1-14

Wei M, X He, N Liu, H Deng (2024). Role of reactive oxygen species in ultraviolet-induced photodamage of the skin. *Cell Div* 19:1-9

XiaoGeng LXGL, CMCM Mei, CXCX Heng, XBXB Ping (2001). Study on extracting citral from *Litsea cubeba* fruits by microwave radiation and determination of citral. *Chem Industr For Prod* 21:87–90

Xing X, H Wang (2021). Anti-asthmatic effect of laurotetanine extracted from *Litsea cubeba* (Lour.) Pers. root on ovalbumin-induced allergic asthma rats, and elucidation of its mechanism of action. *Trop J Pharm Res* 18:1277–1283